Eur. Phys. J. D **34**, 227–230 (2005)
DOI: 10.1140/epjd/e2005-00148-y

THE EUROPEAN PHYSICAL JOURNAL D

Solid solubility in isolated nanometer-sized alloy particles in the Sn-Pb system

J.-G. Lee[a] and H. Mori

Research Center for Ultra High Voltage Electron Microscopy, Osaka University, Yamadaoka, Suita, Osaka 565-0871, Japan

Received 6 September 2004
Published online 13 July 2005 –

Abstract. The finite size effect on both the solid solubility and the thermal expansion coefficient in nanometer-sized lead particles was examined by in-situ transmission electron microscopy. The solid solubility of tin in approximately 12-nm-sized particles of lead at room temperature was evaluated be higher than 30 atomic percent, which is almost ten times higher than that in the corresponding bulk lead. The thermal expansion coefficient of lead increased from 29×10^{-6} K^{-1} for bulk to 38×10^{-6} K^{-1} when the size of particles decreased from ∞ (bulk) to 16 nanometers. The increment of the thermal expansion coefficient with decreasing size of particles suggests the reduction of the cohesive energy and therefore the reduction of the elastic modulus with decreasing size of particles. It is then considered that the suppression of the strain energy in the solid solution may be responsible for the enhanced solid solubility in nanometer-sized alloy particles.

PACS. 61.46.+w Nanoscale materials: clusters, nanoparticles, nanotubes, and nanocrystals – 64.75.+g Solubility, segregation, and mixing; phase separation

1 Introduction

One of the key features of nanometer-sized alloy particles is the solid solubility of solute atoms, since the solubility limit defines the composition range over which a nanometer-sized alloy particle can be present in a single phase and therefore it defines the composition range over which properties of nanometer-sized alloy particles can be modified rather continuously by controlling the concentration of solute atoms. Thus it is of significance to get a fundamental understanding of the solid solubility in nanometer-sized alloy particles. With respect to the solid solubility in embedded nanometer-sized particles, a few experimental results have been reported [1–3]. For example, the solute concentration of individual phases of the two-phase lead-tin inclusions in an aluminum matrix has been examined by Johnson et al. and it is revealed that the concentration is considerably higher than that given in the bulk phase diagram when the size of inclusions is in the range of 10–20 nm [3]. They have suggested that the extended solid solubility in embedded nanometer-sized alloy particles can be partly explained by the Gibbs-Thomson effect. However, it is not evident at this moment whether or not the extended solid solubility comes from the effect. With respect to the solid solubility in isolated nanometer-sized alloy particles, on the other hand, studies have been quite limited. The limitation may come from the difficulty in controlling and measuring size (d) and composition (C) of one isolated particle at the same time in the experiments. Recent remarkable progress in transmission electron microscopy (TEM), however, makes it possible to study the microstructure of an isolated nanometer-sized alloy particle as a function of size (d) and composition (C). With the use of this technique, quite recently, it is revealed that the solid solubility in isolated nanometer-sized alloy particles is significantly higher than that of the corresponding bulk materials in the In-Sn and the Bi-Sn systems [4,5]. Here, it is emphasized that the extension of the solid solubility in isolated nanometer-sized alloy particles is not a metastable extension but a stable extension. However, the reason why the solid solubility can be greatly extended in isolated nanometer-sized alloy particles is not clear.

Based upon this premise, in the present work, the finite size effect on the solid solubility has been examined by in-situ experiments in TEM using particles in the Sn-Pb binary system. Furthermore, in an attempt to consider the mechanism behind the enhanced solid solubility, the size dependence of thermal expansion coefficient has been also examined by in-situ TEM, using lead particles.

2 Experimental procedures

Preparation of nanometer-sized lead particles and subsequent vapor-deposition of tin onto lead particles were carried out using a side-entry holder in a Hitachi HF-2000 type 200 kV high resolution electron microscope (HREM). The holder was equipped with a double-source evaporator

[a] e-mail: jg-lee@uhvem.osaka-u.ac.jp

at its tip. A schematic illustration of the holder can be seen in a previous paper [6]. At the tip set were three spiral-shaped tungsten filaments, the middle one of which was attached with a flake of graphite served as a supporting substrate. Prior to experiment, the flake was baked at 1073 K for 60 s to obtain a cleaned surface. After being baked, the graphite substrate was cooled down to room temperature (RT). Lead was then evaporated from one filament onto the substrate kept at RT, and nanometer-sized lead particles were produced on the edge of graphite. Next, tin was evaporated from the other filament onto the same substrate kept at the same temperature (i.e., RT), to produce Sn-Pb alloy particles. The base pressure in the specimen chamber of this microscope was below 5×10^{-7} Pa. In order to observe the microstructural evolution in a particle associated with alloying, a television camera (GATAN 622SC) and video tape recorder (VTR) system were employed.

To study the thermal expansion coefficient of nanometer-sized lead particles, the lattice parameter of nanometer-sized lead particles was measured over a temperature range from –180 °C to 300 °C using heating and cooling holders with Hitachi H-800 type 200 kV TEM. This TEM was equipped with a different type of a double-source evaporator in the specimen chamber [7]. With the use of the evaporator, both production and observation of nanometer-sized lead particles are possible in the same vacuum chamber without exposing particles to any undesirable atmosphere throughout the experiment. Amorphous carbon films, instead of flakes of graphite, were used as the supporting substrate in these experiments. Preparation of nanometer-sized lead particles was carried out in a similar way as that mentioned above. Quantitative analyses of lattice parameter from the position of Debye-Scherrer rings were performed using imaging plates (IPs) [8], instead of conventional negative films.

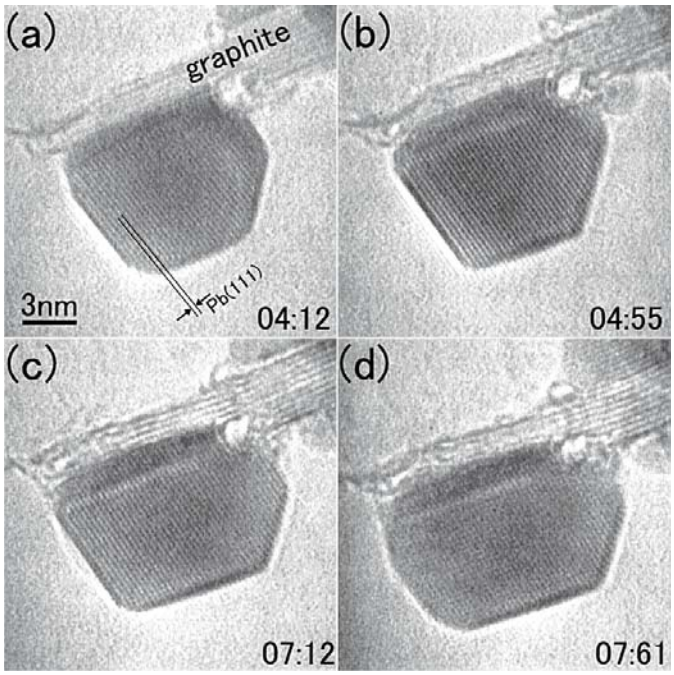

Fig. 1. In situ observation of alloying process of tin into an approximately 10 nm-sized lead particle at room temperature. With continued tin deposition, the particle size increased from approximately 10 nanometers (a) to 12 nanometers (d) in diameter. This increment in size comes from alloying of tin atoms into the lead particle. Estimated tin concentration of the particle in (d) is slightly above 30 at.%. It is noted that the particle remained being a single crystal as shown in (a)–(d), showing the formation of a solid solution.

3 Results and discussion

3.1 Solid solubility of tin in nanometer-sized lead particles

Figure 1 shows a typical sequence of alloying process of tin into a 10-nm-sized lead particle at RT. All micrographs shown in Figure 1 were reproduced from a videotape. The two numbers inserted in each micrograph indicate the elapsed time in units of minutes and seconds. Figure 1a shows an as-produced, pure lead particle on a graphite substrate. The (111) lattice fringes of lead are clearly seen. The same particle after tin deposition is shown in Figure 1b. The diameter of the particle slightly increased by tin deposition. However, the particle remained being a single crystal, indicating the formation of a lead solid-solution. With continued tin deposition, the particle still remained being a single crystal as shown in Figures 1c and 1d. The particle size increased from approximately 10 nanometers to 12 nanometers in diameter by tin deposition, as seen from a comparison of Figure 1a with Figure 1d. The tin concentration in the solid-solution estimated from this size increment amounts to a value slightly higher than 30 atomic percent, which is almost ten times higher than the solubility limit of tin in bulk lead [9]. This experimental result indicates that when tin atoms were vapor-deposited onto a nanometer-sized lead particle at RT, rapid spontaneous alloying of tin atoms into a lead particle took place and as a result a lead solid-solution containing more than 30 atomic percent tin could be formed in an approximately 12-nm-sized particle. This observation clearly indicates that even at RT the atomic mobility is high enough to produce the solid-solution in approximately 10-nm-sized particles. The high atomic mobility in nanometer-sized particles is consistent with our previous results [4,5,10,11]. It is interesting to note here that changes neither in the microstructure nor in the crystallographic orientation of the particle occurred during alloying of tin. This observation indicates that the rapid spontaneous alloying of tin into a lead particle took place not via a melting process but via a purely solid-state process (if the spontaneous alloying took place via a melting process, the microstructure and orientation of the particle would be different between conditions before and after tin deposition). This observation is consistent with our previous work on the spontaneous alloying of copper into nanometers-sized gold particles [12].

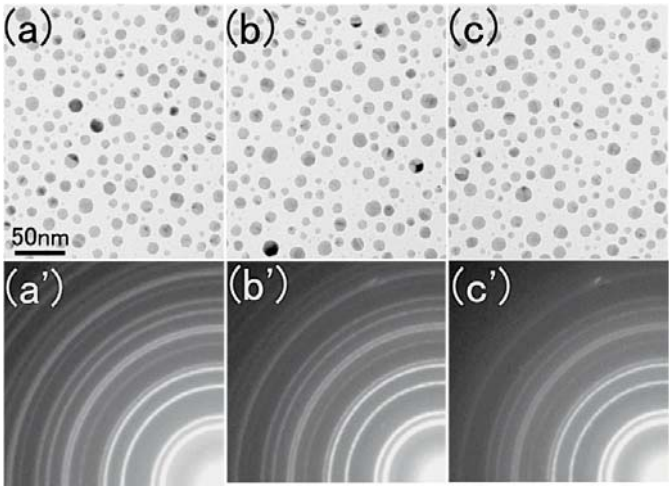

Fig. 2. BFIs ((a)–(c)) and the corresponding SAEDs ((a')–(c')) of lead particles at three different temperatures of –180 °C, –20 °C, and 150 °C.

3.2 Size dependence of thermal expansion coefficient of lead particles

Thermal expansion coefficient of lead particles with two different sizes (16-nm-sized and 40-nm-sized) has been examined by in-situ heating and cooling experiments in TEM. Figures 2a, 2b and 2c show bright field images (BFIs) of lead particles on an amorphous carbon film at –180 °C, –20 °C and 150 °C, respectively. The mean diameter of lead particles was approximately 16 nm and no change in the diameter was noticed even after a high temperature (i.e. 150 °C) observation (The reason for this is that lead particles shown in Figs. 2a–2c had been prepared at a temperature higher than 150 °C, in an attempt to avoid any coalescence among particles during measurements.) Figures 2a', 2b' and 2c' show the corresponding selected area electron diffraction patterns (SAEDs) taken from areas shown in Figures 2a, 2b and 2c, respectively. The Debye-Scherrer rings in Figures 2a', 2b' and 2c' can be consistently indexed as those of a crystal with the face-centered cubic (FCC) structure, which is the same structure as that of pure bulk lead. Intensity profiles of the Debye-Scherrer rings in Figures 2a', 2b' and 2c' are depicted as in Figures 3a, 3b and 3c, respectively. The profile was obtained by digitalizing the data in IPs. As seen from a comparison of Figure 3a with Figures 3b and 3c, peaks of Debye-Scherrer rings shifted left-wards with increasing temperature, which reflected the thermal expansion of lattice parameter. By analyzing the peak-shifts of Debye-Scherrer rings from several different lattice planes, it is confirmed that the lattice spacings varied almost isotropically with temperature. The obtained fractional thermal expansions of 16-nm-sized and of 40-nm-sized lead particles are shown in Figure 4. In Figure 4, the thermal expansion of bulk lead is also indicated [13] for comparison. From Figure 4, it is seen that the thermal expansion coefficient of lead increased from 29×10^{-6} K^{-1} to 38×10^{-6} K^{-1} when the size of particles decreased from ∞ (bulk) to 16 nanometers.

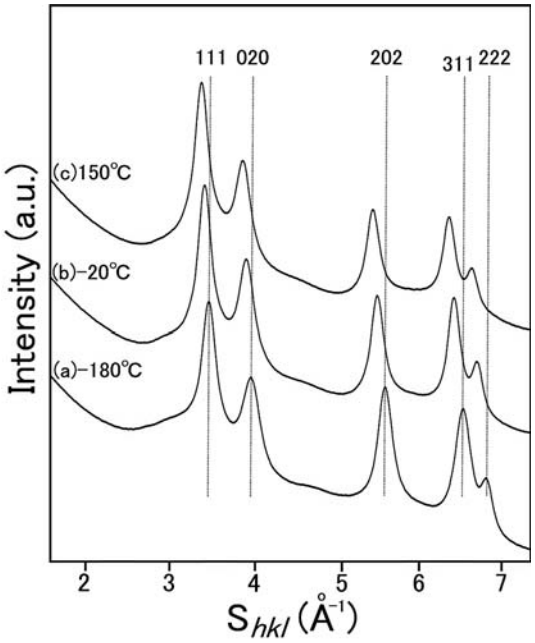

Fig. 3. Profiles (a), (b) and (c) are intensity profiles of Debye-Scherrer rings in Figures 2a', 2b' and 2c', respectively. See text for details.

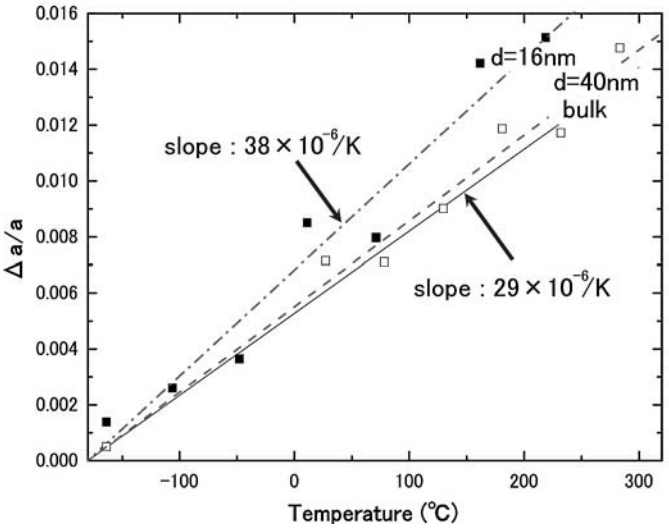

Fig. 4. Thermal expansions of 16-nm-sized and 40-nm-sized lead particles. Thermal expansion of bulk lead is also indicated for reference.

As mentioned above, the thermal expansion coefficient increased with decreasing size of particles. On the other hand, it is known there is a trend that elements with a low cohesive energy possess a high thermal expansion coefficient and vice versa [13]. Then it can be said that the present result indicates the cohesive energy would decrease with decreasing size of particles. This view has been pointed out also in the literature [14–16]. Since it is well

established that elements with a low cohesive energy generally possess a low elastic modulus [17], it seems safe to consider that the elastic modulus would decrease with decreasing size of particles. This decrease in the elastic modulus can lower the strain energy in the solid solution. Namely, the contribution of strain energy to the heat of mixing (i.e. to the formation enthalpy) will become small when the elastic modulus becomes low. This reduction in the formation enthalpy of a solid solution would inevitably bring about the enhancement of the solid solubility, that is, the solubility limit would be increased when the size of particles is reduced. This explanation is in accordance with the present observation that an enhanced solid solubility of tin into lead (i.e. slightly higher than 30 at.% at RT) has been achieved in nanometer-sized particles. However, further study is needed to elucidate the quantitative relationship between the solid solubility and the thermal expansion coefficient in nanometer-sized particles and the authors' research group is now engaged in this study.

4 Conclusions

The finite size effect on both the solid solubility and the thermal expansion coefficient in nanometer-sized lead particles has been examined by in-situ transmission electron microscopy.

Conclusions obtained are given below.

(1) The solid solubility of tin in approximately 12-nm-sized particles of lead at RT was evaluated be slightly higher than 30 atomic percent, which is almost ten times higher than that in the corresponding bulk lead.
(2) The thermal expansion coefficient of lead increased from 29×10^{-6} K^{-1} for bulk to 38×10^{-6} K^{-1} when the size of particles decreased from ∞ (bulk) to 16 nanometers.

This work was supported by "Priority Assistance of the Formation of Worldwide Renowned Centers of Research — The 21stCentury COE Program (Project: Center of Excellence for Advanced Structural and Functional Materials Design)" from the Ministry of Education, Sports, Culture, Science and Technology of Japan. A part of the present work was supported by the Ministry of Education, Sports, Culture, Science and Technology of Japan under a Grant-in-Aid for Scientific Research (Grant No. 15074213 and 15206070).

References

1. S. Hagege, U. Dahmen, Philos. Mag. Lett. **74**, 259 (1996)
2. E. Johnson, A. Johansen, U. Dahmen, H. Gabrisch, S. Hagege, J. Elect. Micros. **48**, 1031 (1999)
3. E. Johnson, A. Johansen, C. Nelson, U. Dahmen, J. Elect. Micros. **51**, S201 (2002)
4. J.-G. Lee, H. Mori, H. Yasuda, Phys. Rev. B **65**, 132106 (2002)
5. J.-G. Lee, H. Mori, H. Yasuda, Phys. Rev. B **66**, 012105 (2002)
6. J.-G. Lee, H. Mori, J. Vac. Sci. Technol. A **21**, 32 (2003)
7. J.-G. Lee, Ph.D. thesis, Osaka University, 2002
8. N. Mori, T. Oikawa, Y. Harada, J. Miyahara, J. Elect. Microsc. **39**, 433 (1990)
9. T.B. Massalski et al., *Binary Alloy Phase Diagrams* (American Society for Metals, Metals Park, OH, 1986)
10. H. Mori, M. Komatsu, K. Takeda, H. Fujita, Philos. Mag. Lett. **63**, 173 (1991)
11. J.-G. Lee, H. Mori, Phys. Rev. Lett. **93**, 235501 (2004)
12. H. Mori, H. Yasuda, T. Kamino, Philos. Mag. Lett. **69**, 279 (1994)
13. J. Emsley, *The Elements* (Oxford University Press, 1989)
14. S.L. Lai, J.Y. Guo, V. Petrova, G. Ramanath, L.H. Allen, Phys. Rev. Lett. **77**, 99 (1996)
15. M. Zhang et al., Phys. Rev. B **62**, 10548 (2000)
16. Q. Jiang, J.C. Li, B.Q. Chi, Chem. Phys. Lett. **366**, 551 (2002)
17. C. Kittel, *Introduction to Solid State Physics* (John Wiley & Sons, Inc., 1996)